

MICROCOPY RESOLUTION TEST CHART
NATIONAL BUREAU OF STANDARDS-1963-A

12



RADC-TR-85-147
Final Technical Report
August 1985

AD-A160 606

LASER PUMPED FREQUENCY STANDARDS

Massachusetts Institute of Technology

Shaoul Ezekiel

DTIC
ELECTE
OCT 25 1985
B

APPROVED FOR PUBLIC RELEASE; DISTRIBUTION UNLIMITED

DTIC FILE COPY

ROME AIR DEVELOPMENT CENTER
Air Force Systems Command
Griffiss Air Force Base, NY 13441-5700

85 10 25 001

This report has been reviewed by the RADC Public Affairs Office (PA) and is releasable to the National Technical Information Service (NTIS). At NTIS it will be releasable to the general public, including foreign nations.

RADC-TR-85-147 has been reviewed and is approved for publication.

APPROVED:



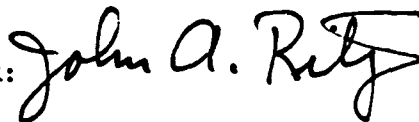
CLARE C. LEIBY, Jr.
Project Engineer

APPROVED:



HAROLD ROTH, Director
Solid State Sciences Division

FOR THE COMMANDER:



JOHN A. RITZ
Plans Office

If your address has changed or if you wish to be removed from the RADC mailing list, or if the addressee is no longer employed by your organization, please notify RADC (ESO) Hanscom AFB MA 01731. This will assist us in maintaining a current mailing list.

Do not return copies of this report unless contractual obligations or notices on a specific document requires that it be returned.

UNCLASSIFIED

SECURITY CLASSIFICATION OF THIS PAGE

REPORT DOCUMENTATION PAGE				
1a. REPORT SECURITY CLASSIFICATION UNCLASSIFIED		1b. RESTRICTIVE MARKING N/A AD-9160 606		
2a. SECURITY CLASSIFICATION AUTHORITY N/A		3. DISTRIBUTION/AVAILABILITY OF REPORT Approved for public release; distribution unlimited		
2b. DECLASSIFICATION/DOWNGRADING SCHEDULE N/A				
4. PERFORMING ORGANIZATION REPORT NUMBER(S) N/A		5. MONITORING ORGANIZATION REPORT NUMBER(S) RADC-TR-85-147		
6a. NAME OF PERFORMING ORGANIZATION Massachusetts Institute of Technology		6b. OFFICE SYMBOL (if applicable)	7a. NAME OF MONITORING ORGANIZATION Rome Air Development Center (ESO)	
6c. ADDRESS (City, State and ZIP Code) Research Laboratory of Electronics Cambridge MA 02139		7b. ADDRESS (City, State and ZIP Code) Hanscom AFB MA 01731		
8a. NAME OF FUNDING/SPONSORING ORGANIZATION Rome Air Development Center		8b. OFFICE SYMBOL (if applicable) ESO	9. PROCUREMENT INSTRUMENT IDENTIFICATION NUMBER F19628-80-C-0077	
8c. ADDRESS (City, State and ZIP Code) Hanscom AFB MA 01731		10. SOURCE OF FUNDING NOS.		
		PROGRAM ELEMENT NO. 61102F	PROJECT NO. 2305	TASK NO. J7
				WORK UNIT NO. 22
11. TITLE (Include Security Classification) LASER PUMPED FREQUENCY STANDARDS				
12. PERSONAL AUTHOR(S) Shaoul Ezekiel				
13a. TYPE OF REPORT Final	13b. TIME COVERED FROM Mar 80 TO Aug 84		14. DATE OF REPORT (Yr., Mo., Day) August 1985	15. PAGE COUNT 24
16. SUPPLEMENTARY NOTATION N/A				
17. COSATI CODES			18. SUBJECT TERMS (Continue on reverse if necessary and identify by block number)	
FIELD	GROUP	SUB. GR.	→ Stimulated resonance Raman effect; Portable Co. in the Class Spectroscopic applications; Microwave and far infrared frequency range	
20	05			
20	08			
19. ABSTRACT (Continue on reverse if necessary and identify by block number) The objective of the research program is an investigation into the feasibility of using the stimulated resonance Raman effect in an atomic beam for time and frequency standards, as well as spectroscopic applications in the microwave to the far infrared frequency range.				
20. DISTRIBUTION/AVAILABILITY OF ABSTRACT UNCLASSIFIED/UNLIMITED <input checked="" type="checkbox"/> SAME AS RPT. <input type="checkbox"/> DTIC USERS <input type="checkbox"/>			21. ABSTRACT SECURITY CLASSIFICATION UNCLASSIFIED	
22a. NAME OF RESPONSIBLE INDIVIDUAL Clare C. Leiby, Jr.		22b. TELEPHONE NUMBER (Include Area Code) (617) 861-3034	22c. OFFICE SYMBOL RADC (ESO)	

DD FORM 1473, 83 APR

EDITION OF 1 JAN 73 IS OBSOLETE.

UNCLASSIFIED

SECURITY CLASSIFICATION OF THIS PAGE

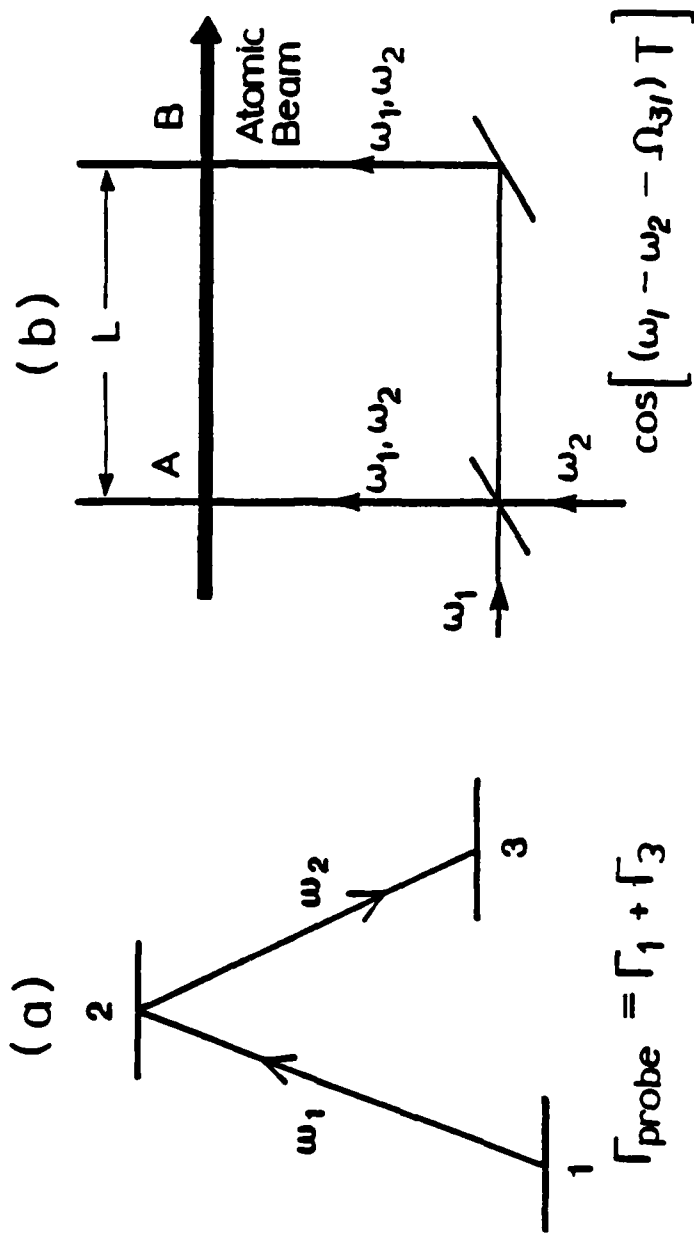


Fig. 1 (a) Schematic of laser-induced resonance Raman interaction.
 (b) Schematic illustrating Ramsey's separated field excitation.

between states 1 and 3. In an atomic beam, the Raman transition linewidth for copropagating laser fields is determined by the decay rates of states 1 and 3, with a negligible contribution from state 2, i.e. the linewidth is limited by laser jitter and transit time since states 1 and 3 are long lived. Moreover, symmetry arguments show that correlated laser jitter (ω_1 and ω_2 jittering together) also does not contribute to the Raman linewidth. Thus, under appropriate experimental conditions, the Raman linewidth is transit time limited, just as for microwaves.

To obtain a small transit time linewidth we use Ramsey's method of separated oscillatory fields, as illustrated in Fig. 1(b), in analogy with conventional microwave techniques. In separated field excitation, an atom-field superposition state created in interaction zone A interferes with a superposition state created in zone B. The resulting interference fringes, which can be observed in zone B only when zone A is present, have frequency widths which are characteristic of the transit time between interaction zones.

III. Experimental Setup

A simplified diagram of our experimental Raman clock setup is shown in Fig. 2. In these preliminary experiments, sodium was used, where states 1 and 3 corresponded to the $F=1$ and $F=2$ hyperfine sublevels of the $3^2S_{1/2}$ ground state which are separated by 1772 MHz, and state 2 was chosen to be

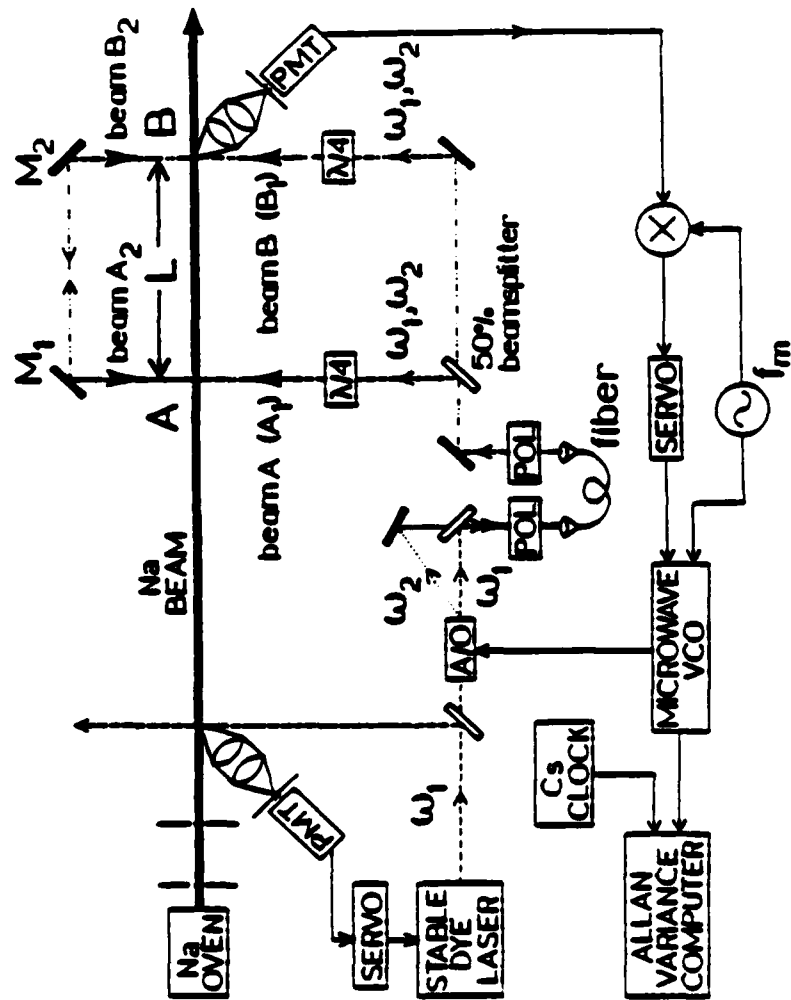


Fig. 2 Experimental Raman clock setup.

the $3^2P_{1/2}(F=2)$ excited state. The sodium atomic beam is produced by heating sodium to 370°C in an oven equipped with a 0.5 mm diameter exit pinhole and a second 0.5 mm diameter collimating pinhole 30 cm downstream, as illustrated in the Fig. 2. The laser at frequency ω_1 is obtained from a single mode dye laser, locked to the $1 \leftrightarrow 2$ transition (D_1), near 5896\AA , using fluorescence from the atomic beam. The laser field at frequency ω_2 was generated directly from that at ω_1 using an acousto optic frequency shifter (A/O), driven with a quartz stabilized microwave oscillator near 1772 MHz. In this way the frequency jitters of ω_1 and ω_2 were correlated so as to obtain a highly stable difference frequency $\omega_1 - \omega_2$. After leaving the A/O the laser beams at ω_1 and ω_2 are combined, passed through a linear polarizer and directed into a polarization preserving single mode optical fiber. At the fiber output the copropagating laser beams are sent through a second linear polarizer followed by a 50% beamsplitter, which produces two optical fields, each having frequencies ω_1 and ω_2 . These two optical fields are then circularly polarized before exciting the atomic beam at the two Ramsey interaction zones, as shown in Fig. 2. The earth's magnetic field is cancelled over the entire interaction length by a set of three-axis Helmholtz coils, not shown.

IV. Lineshape Data

Typical Raman lineshapes obtained with this

experimental setup are shown in Fig. 3. These are obtained by monitoring the fluorescence, induced in zone B, with a photomultiplier while ω_2 is scanned over the $3 \leftrightarrow 2$ transition frequency with ω_1 locked to the $1 \leftrightarrow 2$ transition. The broad feature in Fig. 3(a) corresponds to the 10 MHz wide D_1 transition in sodium. The Raman lineshape (with beam A blocked) appears as three dips in the center of this broad lineshape. There are three dips instead of only one because we applied a 300 mG magnetic Zeeman field along the laser propagation direction. The central dip corresponds to the $m_F = 0, \Delta m_F = 0$ Raman "clock" transition.

These three dips appear with an expanded frequency scale in Fig. 3(b), (beam A unblocked). The narrow feature in the middle of the central dip are Ramsey fringes obtained using an $L=15$ cm Ramsey interaction zone separation. An expanded scan of these fringes appears in Fig. 3(c). The dotted curve superimposed on the data corresponds to the theoretical Ramsey fringe lineshape predicted for a thermal atomic beam velocity distribution. This theoretical lineshape is identical to that predicted for direct microwave excitation.

Optimized fringes for $L = 15$ cm appear in Fig. 4(a). To maximize fringe amplitude, circular polarization was made better than 95% and both laser fields (at ω_1 and ω_2) were adjusted to have 40 μ W of power each with 2mm (FWHM) beam diameters at each of the two interaction zones. At these power levels, the Raman transition saturates and no large

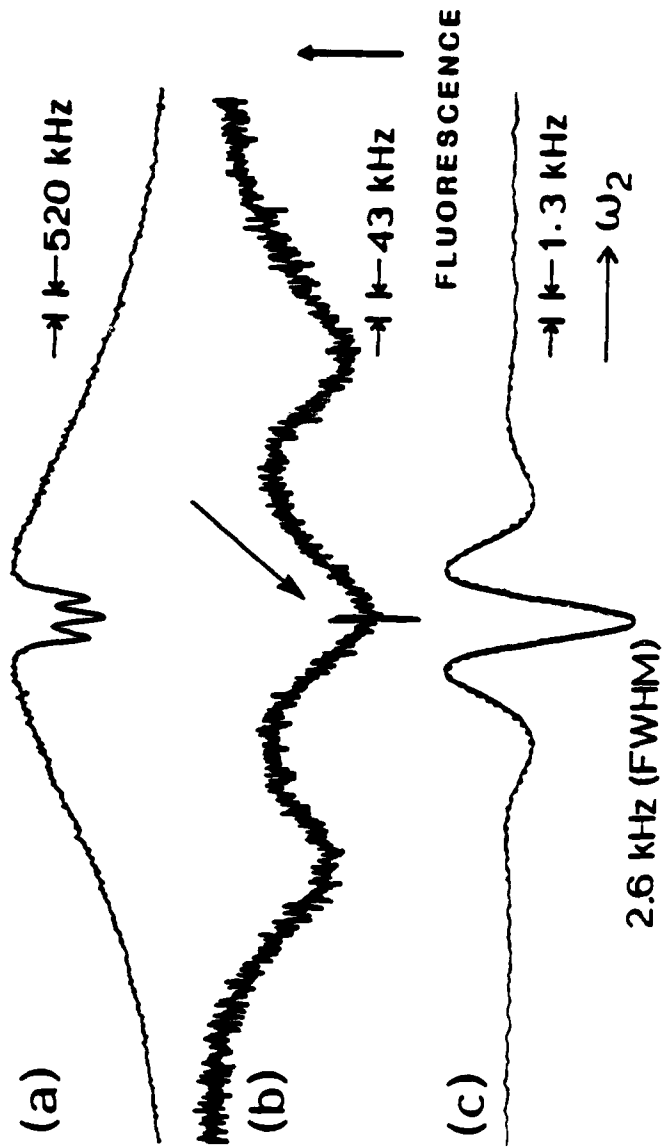


Fig. 3 (a) Resonance Raman interaction in sodium.
 (b) Ramsey fringes for 15 cm interaction zone separation.
 (c) Dotted curve is theory.

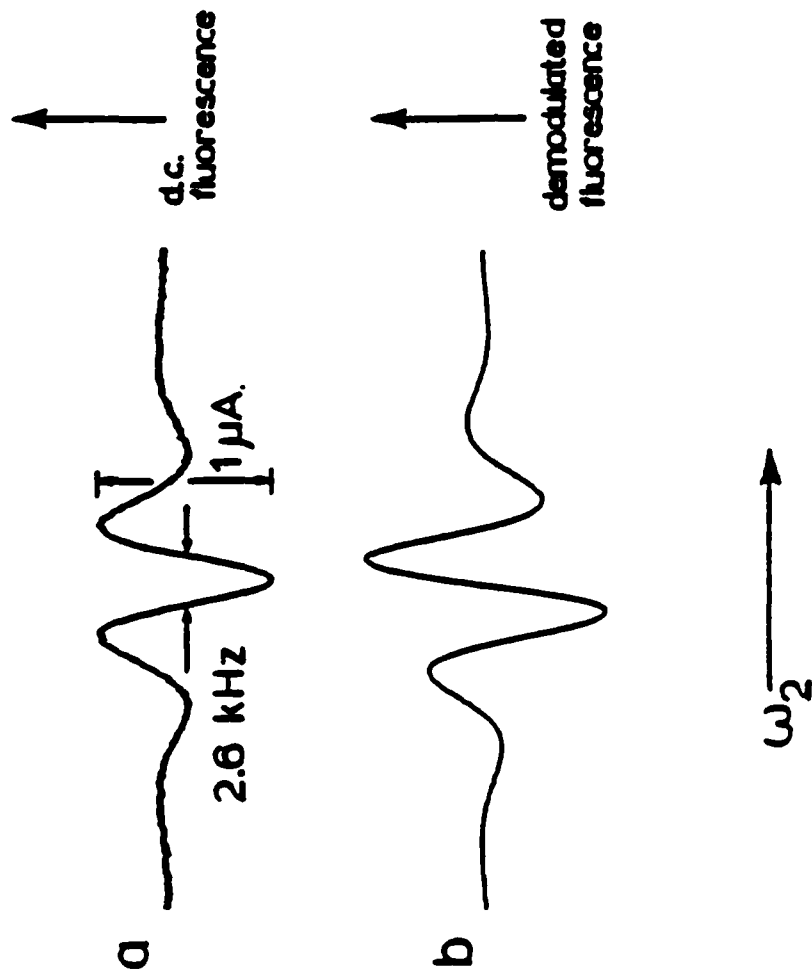


Fig. 4 (a) Typical Raman/Ramsey fringe lineshape for 15 cm Ramsey zone separation.
 (b) Discriminant corresponding to (a).

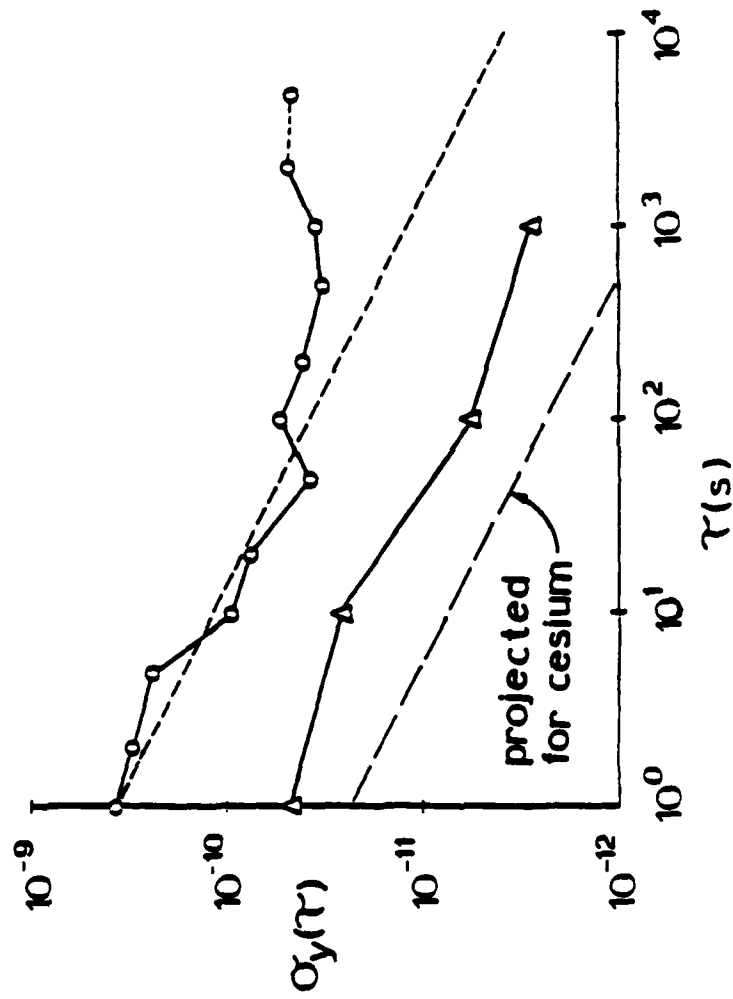
increase in fringe amplitude results for increased laser power. The fringes in Fig. 4(a) have a signal to shot noise ratio of about 1200 for $\tau = 1$ sec.

To stabilize a microwave oscillator to the central fringe of Fig. 4(a), a discriminant is needed. This discriminant, which is shown in Fig. 4(b), is obtained by frequency modulating the microwave source at a rate $f_m = 610$ Hz and demodulating the zone B fluorescence signal with a lock-in amplifier. The output of the lock-in amplifier is then used in a feedback loop to hold the microwave oscillator frequency at the central zero of the discriminant. The stability of this oscillator is then measured by comparing it with a commercial cesium clock, as shown in Fig. 2.

V. Allan Variance

Fig. 5 shows a plot of the measured fractional frequency stability vs. averaging time for the stabilized microwave oscillator. For $\tau = 100$ sec, the stability is about 3×10^{-11} . The dashed line superimposed on the data has a slope of $-1/2$ which is the predicted slope for shot noise limited stability. The data in this plot are close to the shot noise limit. To obtain this data, a Ramsey fringe having a signal to shot noise ratio of 4800 was used. This higher signal to shot noise ratio was obtained by enlarging both the oven and collimating apertures in the atomic beam

Allan variance plot



Δ Portable HP cesium clock

Fig. 5 Plot of measured fractional frequency stability vs. averaging time.

apparatus from 0.5 mm to 1.0 mm diameter, thereby increasing the sodium throughput in the atomic beam.

To compare the stability data of Fig. 5 with conventional cesium clocks, it is necessary to include a factor 16 to account for the higher transition frequency and longer typical transit time of cesium. The lower dashed line in Fig. 5 is the projected stability if cesium were used in place of sodium in our setup with everything else being equal. It is the upper dashed line divided by 16. The triangles are the specifications of a commercial H-P cesium clock ($L = 7$ cm) and are included for comparison. As can be seen, the projected sodium results compare favorably with commercial cesium clocks.

VI. Frequency Error Sources

For averaging times greater than about 100 sec., the fractional frequency stability, Fig. 5, no longer decreases as $\tau^{-1/2}$, indicating the presence of long term frequency drifts.

Preliminary investigations have been made of some of the more important frequency error sources and experimental techniques have been developed to reduce their influence. These error sources include:

(i) Relative Misalignment of Laser Beams

One source of frequency error arises from relative misalignments of the shifted (ω_2) and unshifted (ω_1) laser beams away from copropagating the

interaction regions. In a single interaction region, such errors can be explained in terms of different Doppler shifts for the two laser frequencies. To greatly reduce the effects of relative misalignments the laser beams at both frequencies were made exactly copropagating by directing them into the same single mode optical fiber.

(ii) Optical Phase Shifts

Frequency error can also be produced by any effect that alters the relative phases of the shifted and unshifted laser beams at the interaction regions. Such phase shifts can occur, for example, if there are birefringent optics present and the shifted and unshifted laser beams have different polarizations. To reduce such optical phase shift effects, the polarizations of the shifted and unshifted laser beams are made identical by directing them through a common linear polarizer, as shown in Fig. 2.

(iii) Path Length Phase Shifts

Just as in microwave excitation, changes in optical path length can produce frequency errors in the Raman scheme. We reduced these phase shifts by using standing wave excitation. This is analogous to the use of a cavity in the case of microwaves. For the Raman scheme, however, there

is a possibility of obtaining a higher quality standing wave than is possible using microwaves. For example, microwave cavities have Q's of about 100, while optical cavities can have Q's in excess of 10,000.

(iv) Laser Detuning Shifts

Frequency errors can also occur if the laser, at frequency, ω_1 , is not exactly on resonance with the $1 \leftrightarrow 2$ transition. It was found that such errors could be greatly reduced by using optical pumping techniques. However, laser detuning effects are still under investigation and it is possible that additional techniques will be developed for reducing their influence.

(v) Laser Beam Pointing Stability

In order to achieve good long term stability it is necessary to have constant laser beam intensity and alignment at the interaction regions. In the past, such long term intensity and alignment stability was limited by the mechanical stability and temperature sensitivity of the fiber mounts. To reduce such effects, more rigid fiber mounts having less temperature sensitivity were constructed and a fiber with a larger core diameter was used. Still greater stability was achieved by installing a servo to stabilize the laser power transmitted by the fiber. With these

improvements, a long term laser beam alignment stability of $5 \mu\text{rad}/10^4 \text{ sec}$ and a laser intensity stability of $1\%/10^4 \text{ sec}$ at the interaction regions have been achieved. This leads to expected frequency drifts, related to pointing instabilities, of smaller than $10^{-12}/10^4 \text{ sec}$, for $L = 15 \text{ cm}$.

(vi) Magnetic Field Effects

Changes in the direction or magnitude of stray magnetic fields (including earth's field) present in the laboratory can also cause long term frequency drift. To reduce such drifts, μ -metal shielding was used. In addition, the magnetic holding field (generated by Helmholtz coils inside the shielded region) was also stabilized by using a very low drift current source. With these improvements, the long term frequency drifts due to changes in the magnetic field were reduced to better than $10^{-12}/10^4 \text{ sec}$.

(vii) Other Frequency Error Sources

Additional frequency error sources not yet studied in detail include: (a) atomic beam misalignments, (b) single region slope effects, (c) effects of nearby atomic levels, (d) fluorescence propagating along the atomic beam, (e) optical atomic recoil, (f) second order Doppler shift, etc.

VII. Summary and Suggestions for Future Work

The stimulated resonance Raman effect has been demonstrated in a sodium atomic beam. Ramsey fringes as narrow as 1.3 kHz (FWHM), corresponding to an $L = 30$ cm interaction region separation, have been observed in the second region fluorescence signal. Moreover, the amplitude of these narrow fringes has been observed to be the same as for fringes corresponding to smaller interaction region separations, indicating that transit time is the primary broadening mechanism, just as for microwaves.

A microwave oscillator has been stabilized using Raman/Ramsey fringes corresponding to $L = 15$ cm and fractional frequency stabilities as good as 3×10^{-11} , for $\tau = 100$ second averaging time, have been achieved. These stabilities, which are near the shot noise limit, compare favorably with commercial cesium clock stabilities when differences in transit time and transition frequency are taken into consideration.

Sources of long term frequency drift were partially studied. The major frequency error sources have been identified and experimental techniques have been found to reduce them. It is highly recommended that the study of frequency error sources be continued so that the remaining frequency error sources can also be identified and reduced until the long term stability of the Raman clock becomes comparable to conventional microwave clocks.

It is also recommended that the stimulated resonance Raman technique be used with a cesium atomic beam. Aside from an expected factor of 16 better stability over sodium, there is the possibility developing a much smaller and lighter atomic beam clock by replacing the dye laser with a semiconductor laser. "Off the shelf" GaAs lasers can be obtained, which operate at the 852 nm cesium D_1 transition frequency. Moreover, using the Raman technique, there would be no need for state selection magnets, microwave cavities or hot wire detectors. This would result in less expensive, smaller, lighter and more reliable cesium beam clocks with equal or better stability than commercially available portable clocks.

VIII. Publications

1. J.E. Thomas, S. Ezekiel, C.C. Leiby, Jr., R.H. Picard and C.R. Willis, "Ultrahigh-resolution Spectroscopy and Frequency Standards in the Microwave and Far-infrared Regions using Optical Lasers," *Optics Letters* 6, 298, (1981).

2. J.E. Thomas, P.R. Hemmer, S. Ezekiel, C.C. Leiby, Jr., R.H. Picard and C.R. Willis, "Observation of Ramsey Fringes using a Stimulated Resonance Raman Transition in a Sodium Atomic Beam," *Phys. Rev. Lett.* 48, 867, (1982).

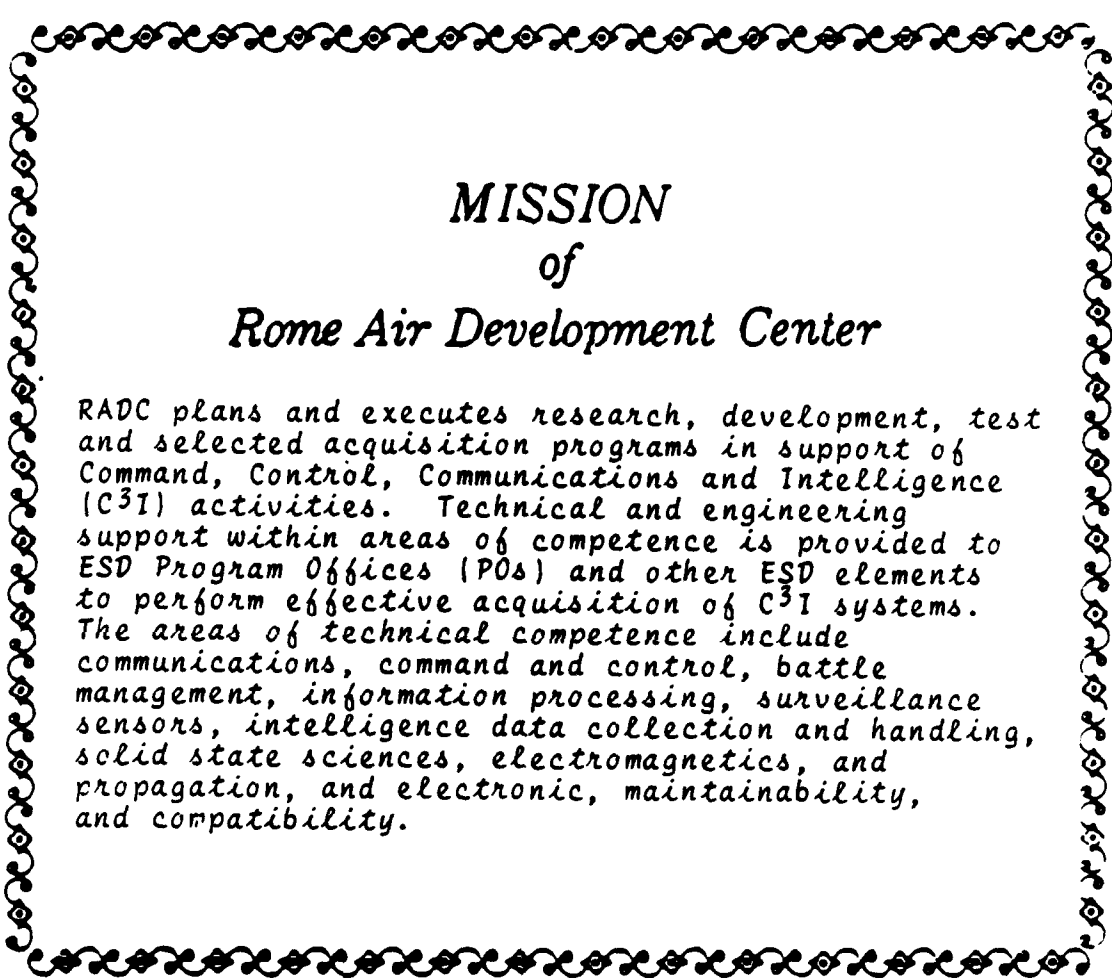
3. P.R. Hemmer, S. Ezekiel and C.C. Leiby, "Stabilization of a Microwave Oscillator using a Resonance Raman Transition in a Sodium Beam," in Laser-Cooled and Trapped Atoms Editor W.D. Phillips, *Natl. Bur. Stand (U.S.) Spec. Publ.* 653 (June 1983) pp. 47-52. Also in Laser-Cooled Trapped Atoms Editor W.D. Phillips, *Progress in Quantum Electronics*, vol. 8, no. 314, 1984, pp.161-164.

4. P.R. Hemmer, S. Ezekiel, C.C. Leiby, Jr., "Stabilization of a Microwave Oscillator using a Resonance Raman Transition in a Sodium Beam," *Optics Lett.* 8, 440 (1983).

5. P.R. Hemmer, S. Ezekiel, C.C. Leiby, Jr., "Preliminary Performance of a Microwave Clock based on a Laser-induced Stimulated Resonance Raman Interaction in a Sodium Atomic Beam," *Proc. International Quantum Electronics Conf., Anaheim* (1984).

IX. Theses Completed

"Precision Studies of Stimulated Resonance Raman
Scattering in Atomic Beams," P.R. Hemmer, Ph.D Thesis 1984.



*MISSION
of
Rome Air Development Center*

RADC plans and executes research, development, test and selected acquisition programs in support of Command, Control, Communications and Intelligence (C³I) activities. Technical and engineering support within areas of competence is provided to ESD Program Offices (POs) and other ESD elements to perform effective acquisition of C³I systems. The areas of technical competence include communications, command and control, battle management, information processing, surveillance sensors, intelligence data collection and handling, solid state sciences, electromagnetics, and propagation, and electronic, maintainability, and compatibility.

END

FILMED

12-85

DTIC